Supplementary Online Material (SOM)

The biting performance of *Homo sapiens* and *Homo heidelbergensis*

Ricardo Miguel Godinho[a,b,c,*], Laura C. Fitton[a,b], Viviana Toro-Ibacache[b,d,e], Chris B. Stringer[f], Rodrigo S. Lacruz[g], Timothy G. Bromage[g,h], Paul O'Higgins[a,b]

[a] *Department of Archaeology, University of York, King's Manor, York, YO1 7EP, UK*

[b] *Hull York Medical School (HYMS), John Hughlings Jackson Building, University of York, Heslington, York, North Yorkshire YO10 5DD, UK*

[c] *Interdisciplinary Center for Archaeology and Evolution of Human Behaviour (ICArHEB), University of Algarve, Faculdade das Ciências Humanas e Sociais, Universidade do Algarve, Campus Gambelas, 8005-139, Faro, Portugal*

[d] *Facultad de Odontología, Universidad de Chile, Santiago, Chile*

[e] *Department of Human Evolution, Max Planck Institute for Evolutionary Anthropology, Leipzig, Germany*

[f] *Department of Earth Sciences, Natural History Museum, London, UK*

[g] *Department of Basic Science and Craniofacial Biology, New York University College of Dentistry, New York, NY 10010, USA*

[h] *Departments of Biomaterials & Biomimetics, New York University College of Dentistry, New York, NY 10010, USA*

[*] Corresponding author.

E-mail address: ricardomiguelgodinho@gmail.com (R.M. Godinho)

SOM S1

This appendix focuses on GM analysis and visualization of modes and magnitudes of deformation (changes in size and shape excluding rigid body rotations and translations) of objects due to loading. Since loading results in changes in both size and shape these are considered together. Here we demonstrate that size and shape distances due to loading (differences between unloaded and loaded objects) scale inversely with size as defined by lengths (e.g., square root of surface area), and directly, with applied force, in identically shaped objects.

Here size and shape coordinates are calculated by multiplying the shape coordinates (from GPA) of each specimen by that specimen's centroid size. This results in the specimens being represented by points in a (size and shape) space that can be thought of as the hemisphere of GPA aligned coordinates with size as an additional dimension. The vector of centroid size (the additional dimension) at any point on the hemisphere can be visualised as passing radially from the centroid of the hemisphere of GPA aligned coordinates (zero size), through that point (centroid size = 1) and beyond it, to infinity (infinite size). When centroid size is 1, the objects lie on the hemisphere of GPA aligned coordinates. This hemisphere is not the same as that arising from translation and rotation with no scaling of landmark configurations (size and shape space described by Dryden and Mardia, 1998). It differs slightly because the eventual rotations of configurations relative to each other without scaling differ from those obtained in full GPA.

In the present application, to deformations arising from FEA, this issue is negligible because variations are extremely small, and both methods generate almost identical results. However, we choose to use rescaled configurations after GPA because this approach preserves the direct relationship between the scaling of size and shape distances and scaling of Procrustes distances (see below).

The scaling relationships we describe here only apply exactly to objects that are identical in shape because as shapes become more different loadings also become different and both of these differences lead to different modes and magnitudes of deformation. Further, for identically shaped models, all linear measures of 'size' (e.g., cube root of volume, square root of area, lengths, centroid size) scale in the same way. This is not the case when models differ in shape and, in this circumstance, scaling relationships differ according to which 'size' variable is used. The extent to which the scaling relationship described here holds when

scaling models with different shapes depends on the degree of shape difference. It is an approximation that depends on the shape difference and chosen size variable.

The scaling relationships also only apply for very small deformations such as arise from FEA analyses using linear elastic models, as in this study. This is because as objects deform, load vectors and resulting modes of deformation also change. This situation of large deformations requires modified FEA analyses (sequentially deforming over small increments), and separate scalings to be computed for each approximately linear increment.

With these caveats noted, we show below that when the same load and constraints are applied to two objects A and B with identical shape but of different size, the ratio of size and shape distances (a and b) between loaded and unloaded forms is the inverse of the ratio of equivalent linear dimensions (a' and b') taken each (e.g. square root of area, length, centroid size); a/b = b'/a'.

This is demonstrated using two examples of 3D models, one of a simple geometric form (a cube; example 1) and the other a complex 3D form (a cranium; example 2). Each example compares magnitudes and modes of deformation among two models that have the same shape but different sizes. These were converted into FE models and in each analysis, identical material properties and boundary conditions were applied to load the models and cause deformation. After solution, landmark coordinates were extracted in each of the models and these were used to visualise and compare global modes of deformation of the models (in size and shape space) due to loading.

Example 1

Two virtual cubes were created, one with 100 mm side length (small cube) and another with 200 mm (large cube), both with a modulus of elasticity of 17 GPa and a Poisson's ratio of 0.3. Two loading regimens were applied, one of 1000 N and another of 2000 N. The results show that, in size and shape space, the small cube deforms (with small error due to the limits of computation) twice as much as the large cube (which has twice the centroid size) under similar loadings (ratio of size and shape distances: 0.009764/0.004867 = 2.006) and that doubling the load doubles the deformation of the cubes (small cube ratio of size and shape distances: 0.019530/0.009764 = 2.000; large cube: 0.009748/0.004867 = 2.003; SOM Fig. S1).

Example 2

Two versions of the *Homo sapiens* cranium were created, one with a voxel side length of 0.35 mm (small cranium) and another with 0.70 mm (large cranium) with identical material properties (Modulus of elasticity of 17 GPa and Poisson's ratio of 0.3). The same boundary conditions were applied, with both glenoid fossae constrained in the X, Y and Z axes and the central incisor in the Z axis. The load applied simulated the action of the temporalis, both masseters and medial pterygoids with a total force of 838.26 N (see SOM Table S1). The results show that the small cranium deforms twice as much (with small error due to the limits of computation) as the large cranium under the same loading (ratio of size and shape distances: 0.179926/0.0899989 = 1.999; SOM Fig. S2).

As such, if two objects differ only in size, but not in shape, the ratio of size and shape distances scales as the inverse of the ratio of 'lengths'. This means that to account for differences in size, the differences in size and shape coordinates (see methods) computed between loaded and unloaded models should be scaled according to the inverse of the ratio of centroid sizes. As noted earlier, this is accurate between identically shaped models, and an approximation when shape differs.

Finally, it should be noted that, although it would be an incomplete analysis, the effects of loading on shape alone may be considered by carrying out GPA with no rescaling to compare the shape of the loaded object with that of the unloaded. In this case, the distances, computed between loaded and unloaded models scale according to the inverse of the ratio of areas or the squares of lengths (e.g., the centroid sizes squared). This is because the size vector in a size and shape analysis results in inflation of (size and shape) distances among larger unloaded and loaded models relative to that between smaller models. When models are scaled to the same centroid size (e.g., centroid size = 1) the distances between unloaded models become zero (they are the same shape) and those between loaded and unloaded models are also scaled, but for each model the scaling is in direct proportion to its size. This has the consequence that while size and shape distances between unloaded and loaded models scale according to the inverse of the ratio of centroid sizes between unloaded models, the resulting Procrustes distances scale with the inverse of the ratio of the squares of centroid sizes.

Supplementary references

Dryden I.L., Mardia, K.V., 1998. Statistical Shape Analysis. Vol. 4. J. Wiley, Chichester.

Slice, D.E., 2001. Landmark coordinates aligned by Procrustes analysis do not lie in Kendall's shape space. Systematic Biology 50, 141-149.

Supplementary figures

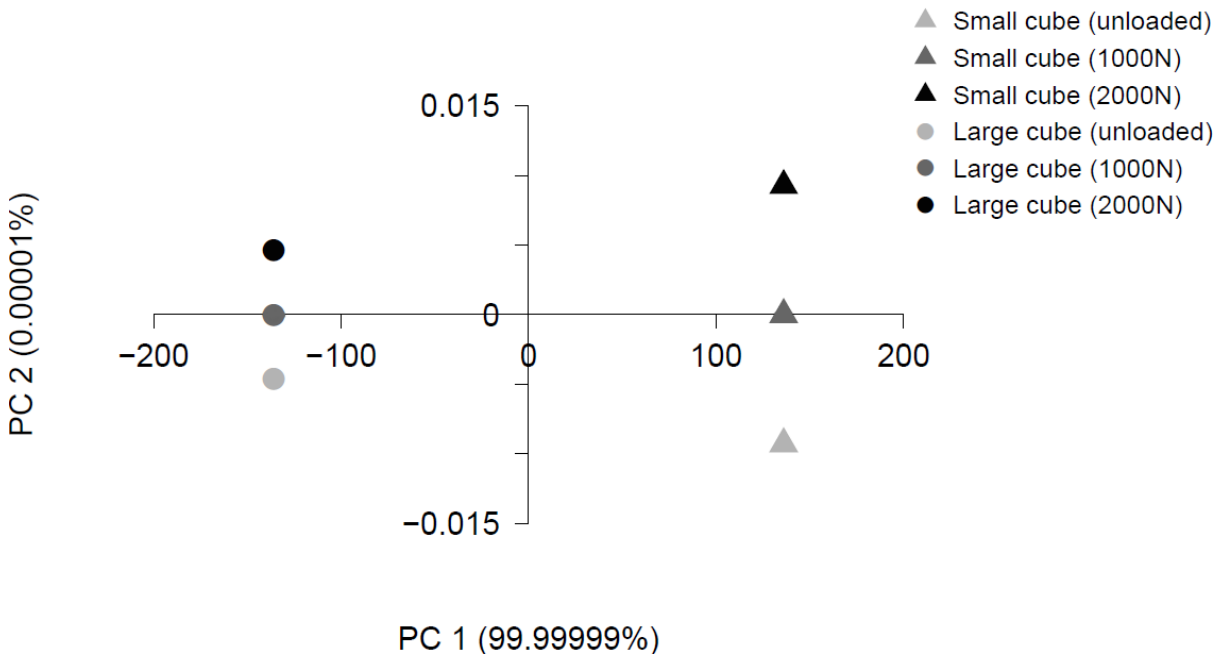

SOM Figure S1. Size and shape space PCA of Cubes 1 and 2 before and after deformation due to loading.

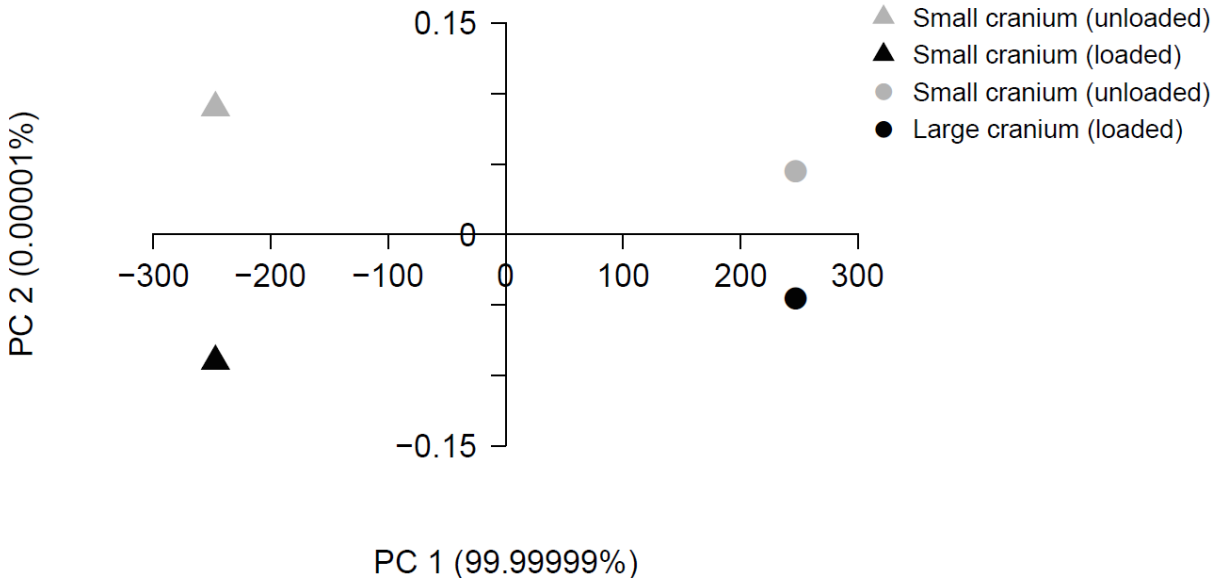

SOM Figure S2. Size and shape space distances of cranium 1 and 2 before and after deformation due to loading.

Supplementary tables

SOM Table S1

Strains experienced by the FE models of *H. sapiens* and Broken Hill at all sampled anatomical points when the same muscle forces are applied. Column 1 identifies numerically all sampled points (landmarks). The location of each landmark is available in Table 1. The remaining columns present the strains experienced by the models of *H. sapiens* and Broken Hill, which, in the latter, are unscaled and scaled according to facial size and muscle force, and according to facial size and bite force.

	Homo sapiens						Kabwe 1 (unscaled)						Kabwe 1 (scaled to muscle force and surface area of face)						Kabwe 1 (scaled to bite force and surface area of face)					
	LI[1]	LI[1]	LP[3]	LP[3]	LM[1]	LM[1]	LI[1]	LI[1]	LP[3]	LP[3]	LP[4]	LP[4]	LI[1]	LI[1]	LP[3]	LP[3]	LP[4]	LP[4]	LI[1]	LI[1]	LP[3]	LP[3]	LP[4]	LP[4]
Landmark	ε1	ε3	ε1	ε3	ε1	ε3	ε1	ε3	ε1	ε3	ε1	ε3	ε1	ε3	ε1	ε3	ε1	ε3	ε1	ε3	ε1	ε3	ε1	ε3
1	1.32	-0.97	1.98	-1.30	2.31	-1.47	0.33	-0.44	0.90	-1.00	1.05	-1.16	0.56	-0.75	1.55	-1.73	1.81	-2.00	0.86	-1.15	2.41	-2.70	3.03	-3.36
2	0.25	-0.55	0.59	-0.80	0.98	-1.05	0.32	-0.12	0.38	-0.14	0.39	-0.18	0.56	-0.21	0.65	-0.24	0.67	-0.30	0.85	-0.32	1.01	-0.38	1.12	-0.51
3	0.15	-0.32	0.84	-2.40	1.67	-4.57	0.79	-2.00	0.86	-2.09	0.93	-2.16	1.36	-3.44	1.49	-3.60	1.61	-3.71	2.09	-5.26	2.32	-5.61	2.70	-6.22
4	5.04	-1.99	3.89	-2.39	5.98	-3.58	3.54	-1.43	3.60	-1.32	3.64	-1.34	6.10	-2.46	6.21	-2.28	6.28	-2.31	9.33	-3.77	9.69	-3.56	10.52	-3.87
5	68.22	-55.48	43.30	-42.69	32.62	-42.56	11.52	-18.45	9.69	-15.08	9.22	-14.60	19.85	-31.78	16.70	-25.97	15.88	-25.15	30.35	-48.61	26.06	-40.53	26.60	-42.14
6	33.60	-26.97	29.82	-12.11	36.64	-17.06	5.55	-13.93	3.38	-5.76	4.27	-6.05	9.57	-23.99	5.82	-9.92	7.36	-10.43	14.64	-36.69	9.09	-15.48	12.33	-17.48
7	426.64	-170.59	308.72	-127.66	290.77	-120.63	90.00	-32.97	78.19	-31.46	74.10	-30.58	155.06	-56.80	134.71	-54.20	127.66	-52.69	237.15	-86.87	210.19	-84.57	213.91	-88.29
8	192.35	-62.30	183.11	-66.47	171.08	-70.47	5.91	-19.17	8.60	-24.66	9.06	-25.50	10.18	-33.02	14.81	-42.49	15.61	-43.94	15.57	-50.50	23.11	-66.29	26.16	-73.62
9	513.59	-200.81	468.78	-183.21	444.02	-173.41	241.71	-80.45	240.76	-80.14	239.00	-79.56	416.42	-138.59	414.78	-138.07	411.76	-137.07	636.89	-211.96	647.18	-215.42	689.97	-229.68
10	318.35	-144.39	320.34	-145.23	330.08	-149.81	73.55	-34.43	75.74	-34.28	77.62	-34.54	126.71	-59.31	130.49	-59.06	133.73	-59.50	193.79	-90.72	203.60	-92.16	224.08	-99.71
11	95.37	-75.51	98.23	-84.07	105.25	-103.09	34.47	-32.56	35.85	-31.73	36.03	-31.76	59.38	-56.09	61.77	-54.67	62.07	-54.72	90.81	-85.79	96.38	-85.30	104.02	-91.69
12	117.24	-210.43	115.64	-227.10	100.49	-197.26	16.82	-37.19	17.61	-36.86	16.47	-34.66	28.98	-64.07	30.34	-63.51	28.38	-59.71	44.32	-97.99	47.34	-99.10	47.56	-100.06
13	332.41	-128.67	228.31	-88.71	157.52	-62.11	63.36	-23.30	82.13	-33.83	85.86	-36.58	109.16	-40.14	141.49	-58.29	147.92	-63.02	166.96	-61.39	220.77	-90.95	247.86	-105.61
14	67.69	-187.15	89.67	-222.00	105.78	-248.00	42.37	-47.17	40.64	-51.24	39.13	-51.75	73.00	-81.27	70.01	-88.27	67.41	-89.16	111.64	-124.30	109.24	-137.74	112.95	-149.40
15	46.20	-22.88	40.70	-20.00	35.26	-17.27	2.91	-1.21	8.97	-3.24	10.24	-3.67	5.01	-2.09	15.45	-5.58	17.63	-6.33	7.67	-3.20	24.11	-8.71	29.55	-10.60
16	122.70	-114.89	55.61	-88.53	54.18	-78.16	37.11	-51.72	42.49	-49.43	48.48	-49.56	63.94	-89.11	73.20	-85.16	83.52	-85.38	97.79	-136.29	114.22	-132.88	139.96	-143.07
17	144.89	-290.67	113.95	-226.75	93.53	-184.75	13.33	-34.82	12.73	-36.77	11.88	-35.61	22.96	-59.98	21.93	-63.34	20.47	-61.36	35.12	-91.74	34.22	-98.84	34.30	-102.81
18	23.05	-14.24	27.08	-16.20	23.64	-14.11	20.55	-15.79	20.14	-13.73	19.51	-13.28	35.40	-27.21	34.69	-23.65	33.61	-22.88	54.13	-41.61	54.13	-36.90	56.32	-38.34
19	55.33	-125.35	61.47	-140.47	54.97	-126.19	15.73	-35.62	21.06	-48.67	20.78	-48.14	27.10	-61.37	36.28	-83.85	35.80	-82.93	41.45	-93.86	56.60	-130.83	59.99	-138.97
20	0.38	-0.25	0.26	-0.14	0.12	-0.17	9.35	-4.10	5.34	-3.78	3.21	-2.79	16.12	-7.06	9.20	-6.51	5.54	-4.80	24.65	-10.80	14.36	-10.16	9.28	-8.04
21	215.39	-509.66	127.43	-301.66	63.98	-147.13	64.46	-174.97	53.87	-144.47	42.00	-111.77	111.05	-301.43	92.80	-248.89	72.36	-192.55	169.84	-461.01	144.80	-388.34	121.25	-322.65
22	186.71	-156.25	30.22	-27.24	19.00	-24.16	203.18	-256.54	27.78	-16.63	13.46	-9.93	350.04	-441.96	47.85	-28.65	23.19	-17.12	535.35	-675.94	74.67	-44.71	38.86	-28.68
23	101.95	-119.17	69.93	-55.72	39.63	-45.40	108.87	-77.61	29.15	-14.26	12.21	-5.60	187.56	-133.70	50.21	-24.57	21.04	-9.65	286.86	-204.49	78.35	-38.33	35.26	-16.17
24	73.88	-50.98	109.81	-77.78	59.48	-69.77	28.16	-11.96	20.01	-24.74	11.81	-4.44	48.51	-20.61	34.47	-42.62	20.35	-7.65	74.19	-31.52	53.79	-66.50	34.10	-12.82
25	9.70	-11.02	46.64	-86.75	68.56	-149.45	55.19	-21.79	54.73	-48.77	53.54	-152.85	95.08	-37.54	94.29	-84.02	92.24	-263.33	145.41	-57.41	147.12	-131.09	154.57	-441.26
26	25.77	-48.51	93.73	-121.63	137.73	-92.81	2.89	-5.60	26.00	-69.84	35.45	-93.26	4.98	-9.64	44.79	-120.32	61.07	-160.68	7.62	-14.74	69.89	-187.74	102.33	-269.24
27	24.96	-9.79	30.99	-13.92	19.24	-34.99	3.07	-1.63	3.80	-1.64	4.24	-1.87	5.28	-2.81	6.54	-2.83	7.30	-3.22	8.08	-4.30	10.20	-4.41	12.23	-5.39
28	106.32	-248.34	31.94	-80.51	43.50	-96.09	57.29	-59.59	29.97	-17.69	15.98	-8.53	98.71	-102.66	51.63	-30.48	27.52	-14.69	150.96	-157.01	80.56	-47.55	46.12	-24.62
29	18.09	-23.01	45.84	-36.88	39.22	-21.51	16.69	-10.50	22.05	-10.98	25.17	-11.49	28.75	-18.09	37.99	-18.91	43.37	-19.80	43.97	-27.67	59.28	-29.50	72.67	-33.17
30	3.22	-7.60	8.43	-17.32	13.49	-26.28	9.92	-4.81	9.75	-5.10	10.39	-4.97	17.09	-8.28	16.80	-8.79	17.90	-8.57	26.13	-12.67	26.22	-13.72	29.99	-14.36
31	0.08	-0.14	0.08	-0.08	0.21	-0.21	4.37	-9.65	2.92	-6.55	2.88	-5.96	7.53	-16.62	5.04	-11.28	4.96	-10.26	11.51	-25.42	7.86	-17.59	8.31	-17.19
32	61.48	-21.10	31.61	-11.00	8.01	-6.85	42.59	-15.49	37.47	-13.64	33.89	-12.33	73.38	-26.69	64.55	-23.49	58.39	-21.24	112.23	-40.82	100.72	-36.66	97.85	-35.59
33	12.84	-6.25	13.43	-6.78	14.57	-7.21	38.31	-12.77	39.43	-13.14	39.65	-13.22	66.00	-22.00	67.93	-22.64	68.31	-22.78	100.95	-33.65	105.99	-35.32	114.46	-38.18
34	4.72	-13.09	4.00	-10.66	5.88	-9.53	10.43	-23.69	10.94	-24.76	10.67	-24.09	17.96	-40.82	18.84	-42.65	18.39	-41.51	27.47	-62.43	29.40	-66.55	30.81	-69.55
35	4.15	-8.87	4.15	-10.18	6.11	-14.39	2.98	-7.59	3.06	-8.69	3.18	-8.77	5.13	-13.07	5.27	-14.97	5.47	-15.11	7.85	-19.99	8.23	-23.37	9.17	-25.32
36	15.99	-9.86	20.77	-20.63	20.18	-21.51	3.74	-5.85	3.03	-4.56	2.86	-4.22	6.44	-10.07	5.22	-7.86	4.93	-7.28	9.85	-15.40	8.14	-12.27	8.26	-12.19

37	54.93	-58.30	43.46	-45.93	38.73	-36.43	22.30	-8.43	19.85	-7.27	18.58	-6.69	38.41	-14.52	34.19	-12.52	32.00	-11.53	58.75	-22.21	53.35	-19.53	53.63	-19.31
38	66.88	-63.57	80.72	-61.68	102.78	-76.72	74.65	-23.04	62.61	-20.38	64.45	-21.06	128.61	-39.69	107.87	-35.12	111.03	-36.28	196.69	-60.71	168.30	-54.80	186.05	-60.79
39	65.03	-132.18	50.86	-117.44	34.96	-85.37	22.27	-30.41	16.16	-27.69	12.72	-23.27	38.36	-52.38	27.84	-47.71	21.92	-40.09	58.67	-80.12	43.44	-74.44	36.72	-67.17
40	161.31	-160.92	116.06	-131.20	53.70	-74.65	48.62	-21.07	39.55	-16.89	31.60	-13.39	83.76	-36.30	68.14	-29.10	54.44	-23.08	128.10	-55.51	106.31	-45.41	91.22	-38.67
41	429.16	-161.79	339.72	-120.17	258.37	-91.43	38.32	-15.17	34.74	-11.19	23.27	-7.60	66.01	-26.13	59.85	-19.27	40.09	-13.09	100.96	-39.97	93.38	-30.07	67.17	-21.94
42	13.07	-5.52	17.51	-7.95	18.55	-8.93	0.06	-0.08	0.08	-0.11	0.08	-0.12	0.11	-0.13	0.14	-0.18	0.14	-0.20	0.17	-0.21	0.21	-0.29	0.24	-0.34
43	34.56	-76.23	39.83	-87.78	39.29	-86.61	15.24	-28.74	17.52	-34.03	18.12	-35.69	26.25	-49.51	30.19	-58.62	31.22	-61.48	40.15	-75.72	47.11	-91.47	52.32	-103.03
44	11.15	-19.63	19.87	-16.74	24.73	-9.44	9.68	-15.78	13.06	-18.63	13.58	-18.05	16.68	-27.18	22.50	-32.10	23.39	-31.10	25.52	-41.57	35.11	-50.09	39.20	-52.11
45	383.67	-167.62	378.65	-163.07	386.39	-165.73	90.34	-31.47	95.51	-31.50	96.17	-31.47	155.63	-54.21	164.54	-54.26	165.68	-54.22	238.02	-82.91	256.74	-84.66	277.62	-90.85
46	104.42	-43.52	77.31	-35.35	64.51	-30.33	4.70	-14.90	3.84	-10.22	3.82	-9.63	8.10	-25.67	6.62	-17.61	6.58	-16.60	12.39	-39.25	10.33	-27.47	11.02	-27.81
47	264.97	-126.44	259.42	-123.86	257.24	-122.95	224.17	-79.54	214.22	-75.85	211.37	-74.79	386.20	-137.04	369.07	-130.67	364.14	-128.85	590.66	-209.59	575.86	-203.89	610.18	-215.91
48	67.53	-30.55	80.97	-36.50	84.89	-38.26	55.28	-29.28	58.23	-29.94	59.41	-30.17	95.24	-50.44	100.32	-51.58	102.35	-51.99	145.67	-77.14	156.52	-80.49	171.50	-87.11
49	131.82	-69.61	132.95	-68.86	86.03	-52.75	36.02	-25.90	35.79	-27.31	35.78	-27.72	62.06	-44.61	61.67	-47.04	61.63	-47.76	94.91	-68.23	96.22	-73.40	103.28	-80.04
50	135.89	-347.18	101.50	-257.47	83.12	-211.06	14.24	-30.10	9.33	-26.80	10.58	-25.90	24.53	-51.85	16.08	-46.17	18.22	-44.62	37.52	-79.30	25.08	-72.05	30.53	-74.77
51	183.91	-67.37	134.01	-49.50	123.93	-45.58	91.30	-33.35	71.15	-27.26	65.99	-25.33	157.29	-57.45	122.57	-46.97	113.69	-43.64	240.55	-87.87	191.25	-73.28	190.52	-73.12
52	42.26	-87.93	47.54	-99.17	61.64	-131.15	39.76	-49.96	35.67	-46.47	34.20	-45.93	68.49	-86.07	61.45	-80.07	58.92	-79.13	104.75	-131.64	95.88	-124.93	98.74	-132.59
53	47.70	-39.28	35.73	-30.39	31.23	-26.19	3.35	-3.34	3.35	-9.20	3.67	-10.42	5.77	-5.76	5.78	-15.85	6.33	-17.95	8.82	-8.80	9.02	-24.73	10.60	-30.08
54	39.50	-57.39	25.33	-41.39	25.06	-42.30	21.73	-45.89	23.69	-40.16	21.76	-35.07	37.43	-79.05	40.81	-69.19	37.49	-60.42	57.25	-120.91	63.68	-107.95	62.83	-101.24
55	49.85	-95.99	31.65	-62.13	25.89	-50.94	10.04	-19.31	6.27	-6.16	6.08	-4.48	17.29	-33.26	10.81	-10.62	10.47	-7.72	26.44	-50.87	16.86	-16.57	17.55	-12.94
56	210.69	-565.35	110.50	-294.98	85.67	-228.10	54.53	-150.67	30.92	-85.19	24.29	-66.83	93.95	-259.57	53.26	-146.76	41.85	-115.13	143.68	-396.99	83.11	-229.00	70.13	-192.92
57	65.30	-77.17	18.45	-28.78	11.89	-19.23	34.76	-26.76	9.21	-5.89	5.00	-3.39	59.89	-46.10	15.86	-10.15	8.62	-5.85	91.60	-70.50	24.75	-15.84	14.44	-9.80
58	5.59	-7.80	2.34	-2.68	1.40	-1.78	25.97	-10.38	10.36	-3.96	5.94	-2.33	44.74	-17.88	17.86	-6.83	10.24	-4.01	68.43	-27.34	27.86	-10.66	17.16	-6.73
59	19.88	-17.17	18.83	-22.98	12.47	-19.72	4.67	-1.96	2.95	-2.76	2.33	-3.12	8.05	-3.38	5.08	-4.76	4.01	-5.37	12.32	-5.16	7.93	-7.43	6.72	-8.99
60	32.57	-84.94	28.17	-60.03	10.37	-27.33	17.27	-7.55	19.68	-7.51	14.46	-6.87	29.76	-13.01	33.91	-12.94	24.92	-11.83	45.51	-19.89	52.90	-20.20	41.75	-19.83
61	18.28	-26.49	15.54	-25.97	13.00	-22.20	3.16	-2.72	3.30	-2.04	3.48	-1.89	5.44	-4.68	5.68	-3.51	6.00	-3.26	8.32	-7.16	8.87	-5.48	10.05	-5.47
62	19.45	-28.63	18.74	-27.24	16.76	-24.01	3.14	-1.73	3.33	-1.78	3.23	-1.75	5.41	-2.99	5.74	-3.07	5.57	-3.01	8.28	-4.57	8.95	-4.79	9.33	-5.04
63	17.81	-46.01	14.80	-38.43	12.42	-32.38	7.16	-16.30	6.22	-14.32	5.88	-13.61	12.34	-28.08	10.71	-24.67	10.12	-23.44	18.87	-42.95	16.72	-38.49	16.96	-39.28
64	157.99	-86.04	235.24	-112.30	272.75	-138.35	72.51	-24.32	94.31	-31.61	97.98	-32.86	124.92	-41.90	162.47	-54.45	168.79	-56.61	191.06	-64.08	253.51	-84.96	282.84	-94.86
65	46.63	-110.51	21.60	-53.98	17.24	-44.60	36.21	-30.96	30.47	-19.28	27.56	-16.17	62.38	-53.34	52.49	-33.21	47.49	-27.85	95.40	-81.58	81.90	-51.82	79.57	-46.67
66	168.61	-134.30	96.62	-72.03	64.51	-52.38	27.97	-21.23	19.41	-13.91	16.43	-11.02	48.19	-36.58	33.44	-23.97	28.30	-18.99	73.70	-55.94	52.18	-37.39	47.43	-31.83
67	111.08	-66.73	45.27	-55.29	16.07	-15.80	30.75	-37.76	18.63	-57.22	14.36	-45.38	52.97	-65.05	32.09	-98.58	24.74	-78.17	81.01	-99.49	50.08	-153.82	41.45	-130.99
Min	0.08	-0.14	0.08	-0.08	0.12	-0.17	0.06	-0.08	0.08	-0.11	0.08	-0.12	0.11	-0.13	0.14	-0.18	0.14	-0.20	0.17	-0.21	0.21	-0.29	0.24	-0.34
Max	513.59	-565.35	468.78	-301.66	444.02	-248.00	241.71	-256.54	240.76	-144.47	239.00	-152.85	416.42	-441.96	414.78	-248.89	411.76	-263.33	636.89	-675.94	647.18	-388.34	689.97	-441.26
Mean	98.38	-91.64	82.10	-73.56	73.75	-65.61	37.04	-30.22	31.23	-24.53	29.56	-24.31	63.81	-52.07	53.80	-42.25	50.92	-41.88	97.59	-79.63	83.95	-65.93	85.33	-70.18
Mean/Mean *H.s.*	—	—	—	—	—	—	0.38	0.33	0.38	0.33	0.40	0.37	0.65	0.57	0.66	0.57	0.69	0.64	0.99	0.87	1.02	0.90	1.16	1.07
SD	116.04	108.59	99.77	73.34	95.75	63.06	48.59	41.50	42.19	25.19	42.25	28.19	83.71	71.49	72.69	43.40	72.79	48.57	128.03	109.34	113.41	67.72	121.96	81.39
T test	—	—	—	—	—	—	0.00014	0.00004	0.00023	0.00000	0.00083	0.00000	0.05024	0.01415	0.06305	0.00329	0.12287	0.01611	0.97013	0.52461	0.92015	0.53275	0.54208	0.71681